A numerical tool for the reconstruction of the physiological kinematics of the glenohumeral joint

Authors: HO Amadi, UN Hansen and AMJ Bull

Departments of Bioengineering and Mechanical Engineering Imperial College London, United Kingdom

Abstract

The aim of this study was to develop and test a robust approach to apply a joint coordinate system (JCS) to imaging datasets of the GHJ and to reconstruct the kinematics with six degrees of freedom (DOF) in order to investigate shoulder pathologies related to instability. Visible human data was used to reconstruct bony morphology. Landmarks were used to define axes for body-fixed Cartesian coordinate frames on the humerus and scapula. These were applied to a three-cylinder open chain JCS upon which the humeral 6 DOF motions relative to the scapula were implemented. Software was written that applies 6 DOF input variables to rotate and translate the nodes of the surface geometry of the humerus relative to the scapula in a global coordinate frame. The instantaneous relative position and orientation of the humerus for a given set of variables was thus reconstructed on the bone models for graphical display. This tool can be used for graphical animation of shoulder kinematics, demonstrating clinical assessments, and allowing further analysis of the function of tissues within the joint.

Keywords: glenohumeral kinematics, JCS, shoulder motion

Introduction

Advanced computer-assisted surgical planning at the shoulder relies on adequate modelling of the functional behaviour of the associated tissues. One of the keys to achieving this is the description and measurement normal kinematics. The glehohumeral joint (GHJ) has six degrees of freedom (6DOF) and surgical interventions to restore shoulder joint stability as a result of pathologies or traumatic sporting injuries do not always successfully restore anatomical joint mobility **[1]**. GHJ motion has historically been viewed in the literature as a simple ball-and-socket assembly with three-degrees of rotational freedom **[2, 3, 4, 5, 6]**. This description disregards joint laxity which is an important clinical component of GHJ motion **[7, 8, 9]**. Functional laxity of the GHJ allows for controlled minimal translations of the humeral head during overall shoulder motion. Pathological laxity, that includes subluxations, must also be able to be described and measured.

The International Society of Biomechanics (ISB) proposed a JCS based on various anatomical landmarks **[10, 11]**; others have proposed alternatives **[12]**. The choice of landmarks from the ISB recommendations or the other studies results in coordinate frames that are not easy to relate to the clinical situation **[13]**. Therefore, the aim of this study was to propose and test a JCS for the GHJ the axes of which are closely aligned to standard planes in the anatomical position.

Methodology

Glenohumeral movement during function was gyroscopically viewed from the perspective of ‘a mobile humeral motion relative to a stationary scapula’. It was therefore needful to establish a scapular positional identity in space as well as the instantaneous orientation and positional identities of the mobile humerus. The approach taken was to establish two separate coordinate frames for the humerus and scapula. The functional interaction of the frames yields the GHJ coordinate system (the JCS). Mathematically, each of the humeral and scapular frames

contributes one of its principal axes as a representation for the JCS formation. These three frames are described below.

The Humeral Coordinate Frame: The three orthogonal axes of the frame were established using the axis through the centre of the humeral canal ($\boldsymbol{H_x}$) and a line joining the centre of humeral head to the greater tubercle **[12, 14]**. A custom-written numerical algorithm that fitted different least-square (LS) geometric shapes to an given data was developed. Axial cross-sections of the humerus were segmented, reconstructed and applied to the custom-written software and this fitted LS ellipses on each cross-section. This also quantified the centre of each fitted ellipse and an LS line through the centres to produce the humeral canal axis. The centre of the humeral head (HH) was quantified as the centre of a LS sphere fit on the points representing the HH. $\boldsymbol{H_x}$ was the first of the three principal axes of the humeral coordinate frame. The cross-product between $\boldsymbol{H_x}$ and the greater tubercle line produced the second principal axis ($\boldsymbol{H_y}$) of the frame, directed anteriorly. The third axis ($\boldsymbol{H_z}$), directed medio-laterally was the cross-product between ($\boldsymbol{H_x}$) and ($\boldsymbol{H_y}$).

The Scapular Coordinate Frame: A clinically optimal scapular coordinate frame as defined in the literature was applied **[13]**. Briefly, this consists of a medial-lateral axis ($\boldsymbol{S_z}$) quantified through the centre of the root of the scapular spine; an anteriorly directed axis ($\boldsymbol{S_y}$) quantified as the vector product of ($\boldsymbol{S_z}$) and a line through the centre of the ridge of the scapular lateral border. The third axis ($\boldsymbol{S_x}$) is mutually orthogonal to these and is directed inferior-superiorly.

The Joint Coordinate System: The JCS was quantified for the description of the humeral motion relative to the scapula (Figure 1). The humeral activities of the JCS were represented using the inferior-superior axis ($\boldsymbol{H_x}$) of its frame while the scapular activities were represented using the medial-lateral axis ($\boldsymbol{S_z}$) of its frame. The interaction of the representative axes in relative motion was quantified to produce the third axis of the JCS called the 'floating axis' ($\boldsymbol{F}$) **[11]**. The floating axis is mutually

orthogonal to the representative axes. This was quantified as the vector product between ($\boldsymbol{H_x}$) and ($\boldsymbol{S_z}$). Humeral abduction-adduction, flexion-extension and internal-external rotation were accomplished about axes ($\boldsymbol{F}$), ($\boldsymbol{S_z}$) and ($\boldsymbol{H_x}$), respectively. Humeral anterior-posterior, medial-lateral and compression-distraction translations were accomplished along axes ($\boldsymbol{F}$), ($\boldsymbol{S_z}$) and ($\boldsymbol{H_x}$) respectively. The humeral rotation centre and the origin of the JCS coincided at the centre of the sphere-fit on humeral head.

Testing the JCS

The female dataset of the Visible Human Project [VHP, National Library of Medicine, Rockville Pike, Bethesda, MD 20894] (slice thickness: 0.33 mm) was used to reconstruct the geometries of the right humerus and scapula as a collection of surface nodes. The constituent nodes of each volume of the humerus or scapula were recognisable vectors in space relative to the original scanning (global) coordinate frame of the medical image. The nodes were inter-webbed in a triangular mesh with each node having a unique interconnectivity number that identified its immediate neighbours [Figure 2]. An algorithm was developed for the transformation of a given node vector from one spatial position and orientation in 3-D space to another (Figure 3). This was designed to apply a stepwise operation of pre-prescribed 6DOF variables of the JCS. The algorithm was translated into a subroutine for the transformation of the humeral volume to obtain a new instantaneous position of the volume relative to the scapula. This was achieved through a loop of iterative process that imposed the prescribed 6DOF variables on all the constituent node vectors of the humeral volume whilst maintaining their nodal inter-connectivity information. Thus a new position and orientation of the corporate volume was achieved.

<u>Application of Algorithm to a Specific Dataset:</u>

Software was written that applied the quantified JCS axes as defined previously and an input file of sets of the 6 variables of DOF of the joint. The variables were anterior, superior and lateral translations in (mm) and abduction, flexion and external rotation in (°). The approach used here is to rotate and translate each node within the geometrical dataset by the kinematic variables. The software opens the default file containing the reconstructed humeral volume, rotates and translates its nodes such that the humeral coordinate frame coincides with that of the scapular and the HH just touching the glenoid. This aligned position defines the neutral point from which the JCS variables are measured. For each nodal vector, the software applies the transformation subroutine and each JCS axis in turn to implement the appropriate rotation and translation upon it. The imposition of a set of 6DOF variables upon all the nodal vectors and the restoration of the original node-to-node interconnectivity thus produce a new instantaneous position and orientation of the humerus relative to a stationary scapula. Each set of 6DOF variables in the input file produces one instantaneous position of the humeral volume. All the instantaneous position files describing a humeral motion relative to the scapula were displayed as individual images. Movie Maker software [Version 2.0 beta, Microsoft Corporation, Seattle, USA] was applied to arrange the images to animate the kinematics of the reconstructed humerus relative to a stationary scapula.

Sequence Independence: The simulation of instantaneous physiological positions involving combinations of humeral motion, such as cocked phase of throwing “abduction plus extension”, was by definition sequence independent. This implied achieving the same final instantaneous position irrespective of the order of applying the six DOF. The ability of the developed tool to achieve this was tested.

Results

Simulations and animations of the clinical definitions of translations (medial-lateral, anterior-posterior and axial compression-distraction) from the aligned neutral position

were realised; and those of the clinical definitions of adduction-abduction, flexion-extension and internal-external rotations, were also realised (Figure 4). Figure 5 shows the result of changing the sequence of humeral rotations of the model. This is illustrated with a GHJ orientation describing an instant during throwing (using 45° flexion and 60° abduction).

Discussion

In this study we have successfully developed a model to reconstruct 6 DOF GHJ kinematics and demonstrated its sequence independency.

The literature proposes various techniques for defining and describing joint motions **[1, 2, 11]**. The description and use of a particular coordinate system among researchers have so far depended on the individual's choice and convenience as it affected the particular study at hand. This has led to models that compromised the clinical definition of the GHJ by either reducing it to a ball and socket system or constraining its freedom in some way to achieve the study purpose **[1, 2, 4, 5, 6]**. All versions of the kinematics systems have attempted to make use of landmarks on the surface of the humerus and the scapula to establish a repeatable sense of humeral motion with respect to the scapula, or vice versa. Some systems were made more complex by the incorporation of other joints of the upper extremity in their models. Notable among these descriptions is the scapulohumeral rhythm model of Charlton **[5]**. Another is the model due to Van der Helm **[2]**, which extends linkage definitions up to the sterno-clavicular joint of the thorax region.

In the present study, the graphical simulation of the relative positions of the bones at different instants for a large range of motion was implemented using the most robust idea of a JCS as discussed by the ISB, recommended for other joints of the extremities, but not actually recommended by them for the GHJ **[10]**. In the so-called

Paradox of Codman **[15]**, some combinations of humeral motion such as ‘abduction plus flexion’ result in different final humeral position if the order of the same motion were changed to ‘flexion plus abduction’ (see Figure 5) **[16, 17]**. Unlike the sequence dependent Euler-Cardan approach, this model’s ability to demonstrate sequence independency ensures accuracy in repeatability of complex physiological motions of the joint such as seen in Codman’s Paradox **[15]**.

The present approach to manoeuvring the humerus relative to the scapula allows the simulation of various kinds of GHJ motion using the same model. This therefore makes it a potential tool for application in the study the kinematics of the attaching soft tissues during various functional manoeuvres of the GHJ. It can easily be adapted for patient specific study of an individual case during surgical planning by applying the actual bone sets of the patient to the model. A further study is focusing on applying this tool to a recent mathematical model **[18]** to study how the ligaments and capsule may respond during shoulder function.

Figure Legends

Figure 1: Glenohumeral joint coordinate system

Figure 2: Reconstructed humeral volume showing a web of inter-connected nodes

Figure 3: Position vector transformation. Mathematical implementation of a situation involving both translation and rotation of a node from point 'p_1' to point 'p_3' was accomplished using a step-by-step rule [described in full in Amadi (2006)]. φ is angular displacement to move from p1 to p2 while k is translation from p2 to p3.

(1) Angle $\theta = \arccos[(\boldsymbol{u}_{op1}) \cdot (\boldsymbol{u}_{sz})]$

(2) The distance, $|os| = |op_1|\cos\theta$

(3) The vector, $(\boldsymbol{os}) = |os|(\boldsymbol{u}_{sz})$

(4) The vector, $(\boldsymbol{sp_1}) = (\boldsymbol{op_1}) - (\boldsymbol{os})$. This is normal to the m-l line with direction cosines or unit vector, $\boldsymbol{u}_{sp1}$

(5) The orthogonal n-n', is $(\boldsymbol{u}_{nn}) = (\boldsymbol{u}_{sz}) \times (\boldsymbol{u}_{sp1})$

(6) The distance, $|sp_1| = |sp_2|$

(7) The vector, $(\boldsymbol{sp_1}) \parallel (\boldsymbol{qp_2})$

(8) Therefore, $|sq| = |sp_1|\cos(90-\varphi)$ or $|sq| = |sp_1|\sin\varphi$

(9) The vector $(\boldsymbol{sq}) = |sq|(\boldsymbol{u}_{nn})$

(10) The distance $|qp_2| = |sp_1|\cos\varphi$

(11) Following from equation (7), $(\boldsymbol{qp_2}) = |qp_2|(\boldsymbol{u}_{sp1})$

(12) The vector, $(\boldsymbol{sp_2}) = (\boldsymbol{sq}) + (\boldsymbol{qp_2})$

(13) Due to rotation, $(\boldsymbol{op_2}) = (\boldsymbol{os}) + (\boldsymbol{sp_2})$

(14) Therefore, with the translation component, the final transformed position vector is $(\boldsymbol{op_3}) = (\boldsymbol{op_2}) + k(\boldsymbol{u}_{sz})$

Figure 4: Translations: (a) medial-lateral (b) anterior-posterior (c) compression-distraction Rotations: (d) adduction-abduction (e) flexion-extension (f) internal-external. These demonstrate the ability of the developed numerical tool to graphically reconstruct and implement a given range of humeral motion relative to a stationary scapula based on the input of a set of JCS variables describing the GHJ motion. Transparent shading traces humeral instantaneous relative positions for the range of motion.

Figure 5: Sequence independence demonstration. S1,S2: Sequences 1 and 2; Right hand side images demonstrate the final humeral orientation relative to the stationary scapula. This remained the same irrespective of the motion sequence.

References

1 **Novotny, J., Beynnon, B.,** and **Nichols, C.** Modeling the stability of the glenohumeral joint during external rotation. Journal of Biomechanics, 2000, **33**, 345-354.

2 **Van der Helm F.** A standardized protocol for motion recordings of the shoulder. In Veeger HEJ, Van der Helm FCT, Rozing PM, editors. Proceedings of the First Conference of the International Shoulder Group, 1997, Maastricht, Netherlands.

3 **Fung, M., Kato, S., Barrance, P., Elias, J., McFarland, E., Nobuhara, K.,** and **Chao, E.** Scapular and clavicular kinematics during humeral elevation: A study with cadavers. Journal of Shoulder and Elbow Surgery, 2001, **10**, 278-285.

4 **De Groot, J.,** and **Brand, R.** A three-dimensional regression madel of the shoulder rhythm. Clinical Biomechanics, 2001, **16**, 735-743.

5 **Charlton, I.** A model for the prediction of the forces at the glenohumeral joint. PhD Thesis, 2003, University of Newcastle upon Tyne, United Kingdom.

6 **Buchler, P.,** and **Farron, A.** Benefits of an anatomical reconstruction of the humeral head during shoulder arthroplasty: a finite element analysis. Clinical Biomechanics, 2004, **19**,16-23.

7 **Senavongse, W., Farahmand, F., Jones, J., Bull, A.,** and **Amis, A.** Quantitative measurement of patellofemoral joint stability: force-displacement behavior of the human patella in vitro. Journal of Orthopaedic Research, 2003, **21**, 780-786.

8 **Gagey, O.,** and **Gagey, N.** The hyperabduction test. An assessment of the laxity of the inferior glenohumeral ligament. Journal of Bone and Joint Surgery Br, 2001, **82-B**, 68-74.

9 **Hawkins, R.,** and **Hawkins, R.** Failed anterior reconstruction for shoulder instability. Journal of Bone and Joint Surgery Br, 1985, **67-B**, 709-714.

10 **Wu, G., van der Helm, F., Veeger, H., Makhsous, M., Roy, P., Anglin, C., Nagels, J., Karduna, A., McQuade, K., Wang, X., Werner, F.,** and **Buchholz, B.** ISB recommendation on the definitions of joint coordinate systems of various joints for the reporting of human joint motion-Part II:shoulder, elbow, wrist and hand. Journal of Biomechanics, 2005, **38**, 981-992.

11 **Grood, E.,** and **Suntay, W.** A joint coordinate system for the Clinical Description of Three-Dimensional Motions: Application to the knee. Trans ASME Journal of Biomechanical Engineering, 1983, **105**,136-144.

12 **Hill, A.** Passive stability of the glenohumeral joint. PhD Thesis, 2006, Imperial College, University of London, United Kingdom.

13 **Amadi, H., Hansen, U., Wallace, A.,** and **Bull, A.** A scapular coordinate frame for clinical and kinematic analyses. Journal of Biomechanics, 2008, **41**, 2144-2149.

14 **Amadi, H.** Glenohumeral joint kinematics and ligament loading. PhD Thesis, 2006, Imperial College, University of London, United Kingdom.

15 **Codman, E.** The shoulder: Rupture of the supraspinatus tendon and other lesions in or about the subacromial bursa, 2nd ed, 1934, T Todd Co, Boston, USA.

16 **Cheng, P.** Simulations of Codman's paradox reveals a general law of motion. Journal of Biomechanics, 2006, **39**, 1201-1207.

17 **Stepan, V.,** and **Otahal, S.** Is Codman's paradox really a paradox? Journal of Biomechanics, 2006, **39**, 3080-3084.

18 **Amadi, H., Sanghavi S., Kamineni S., Hansen, U.** and **Bull, A.** Capsular insertion plane on the proximal humerus. Journal of Anatomy, 2008, **212**, 863-867.

Figure 1

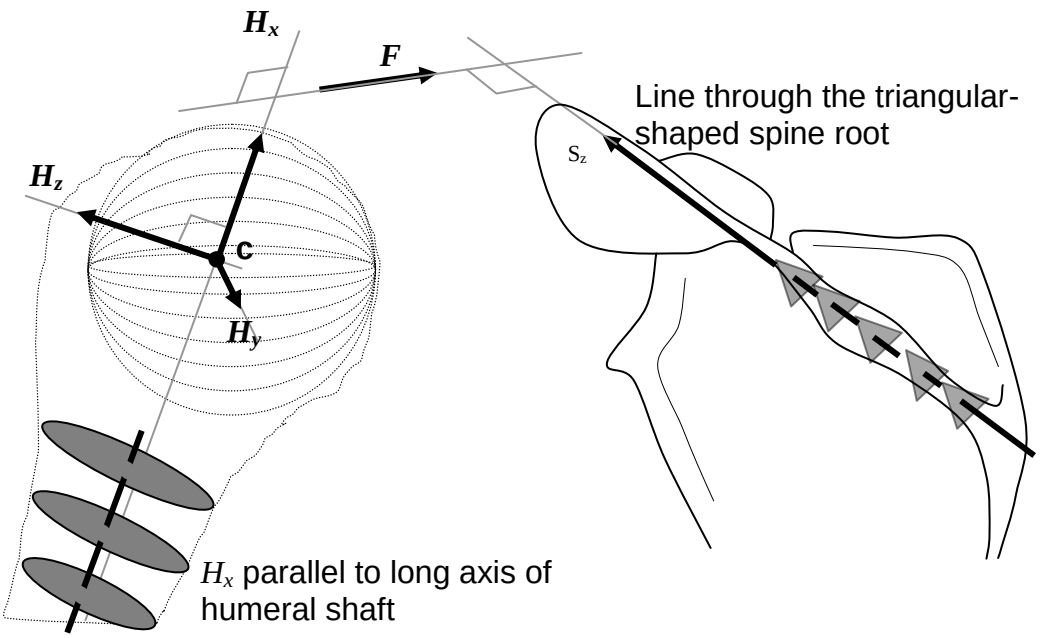
H_x
F
H_z
C
H_y
Line through the triangular-shaped spine root
S_z
H_x parallel to long axis of humeral shaft

Figure 2

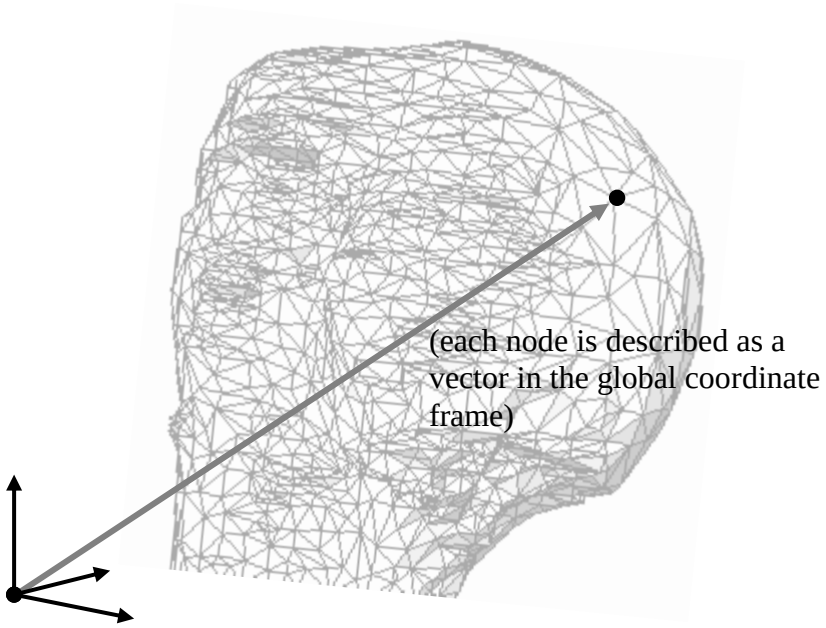
(each node is described as a vector in the global coordinate frame)
Global coordinate frame

Figure 3

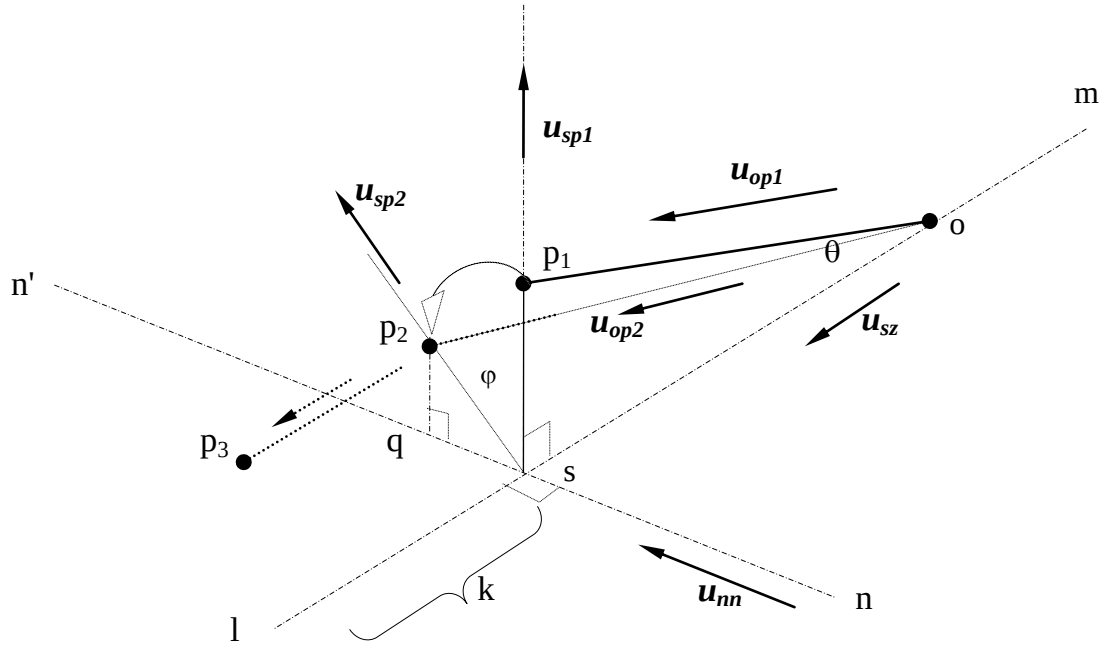

Figure 4

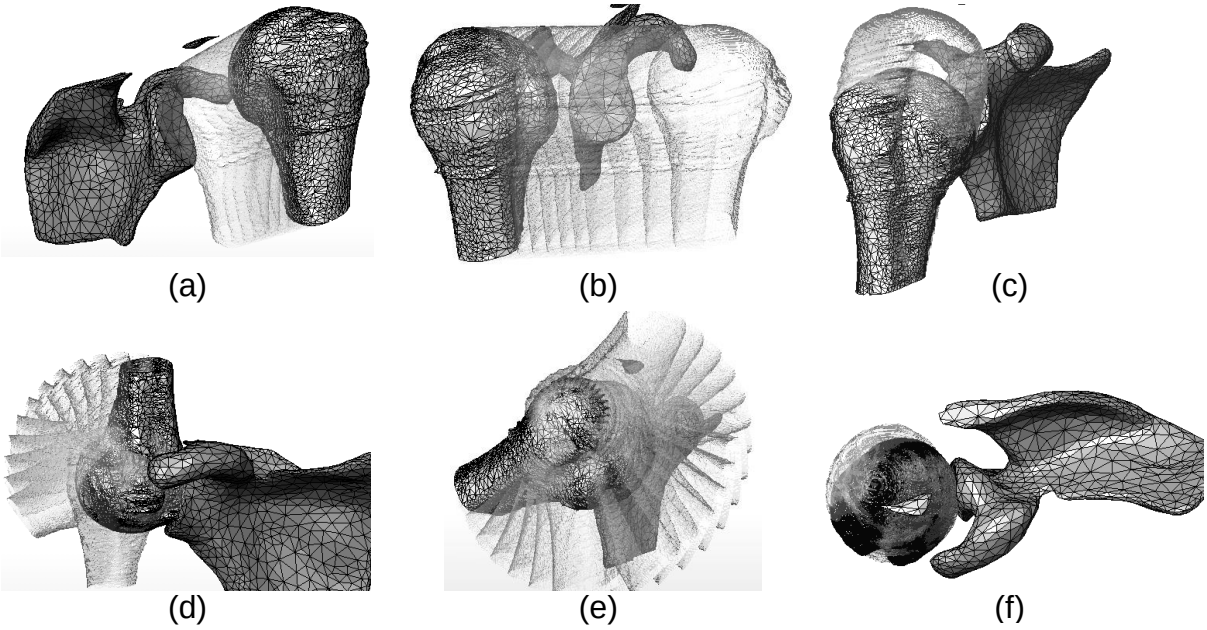

Figure 5

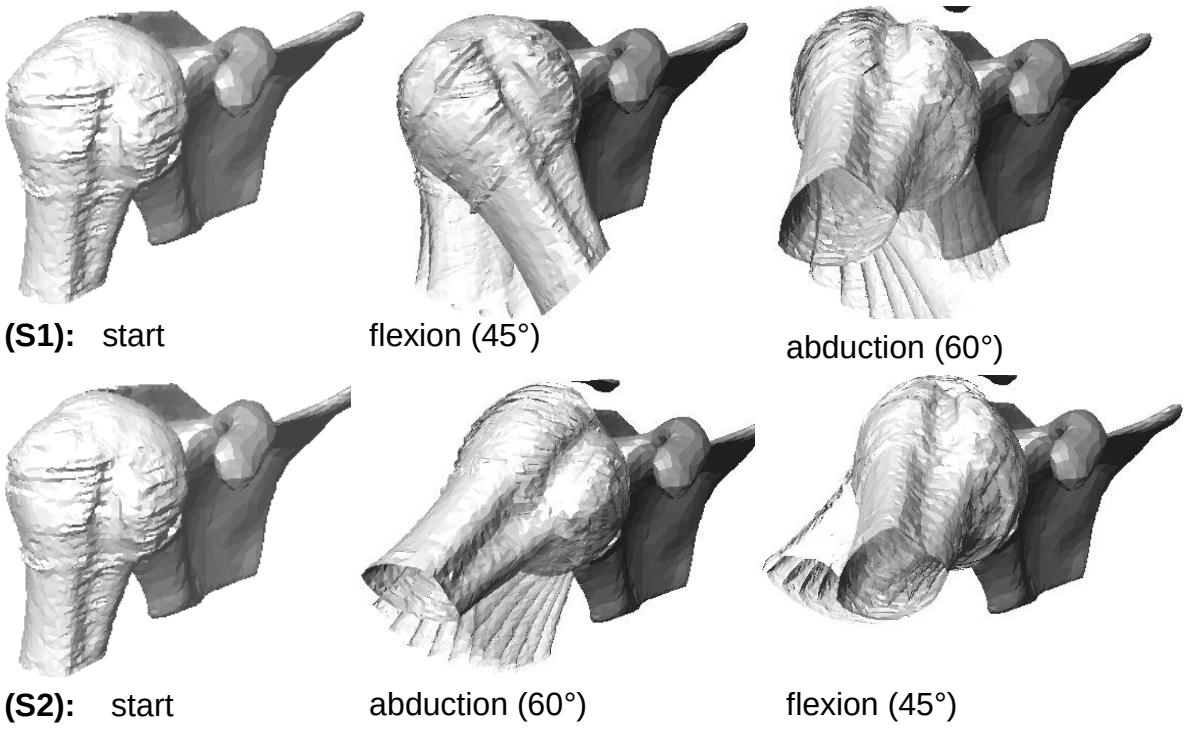
(S1): start
flexion (45°)
abduction (60°)
(S2): start
abduction (60°)
flexion (45°)